Synthesis and properties of an N-substituted polypyrrole with liquid crystalline moieties

Moayad Almasri, Peter J.S. Foot[*], John W. Brown and Jacqueline A. Clipson

School of LSPC, SEC Faculty, Kingston University, Penrhyn Road, Kingston-upon-Thames, Surrey. KT1 2EE, UK

*Corresponding Author. E-mail: p.j.foot@kingston.ac.uk

SUMMARY

The synthesis and characterisation of a pyrrole monomer substituted at the N-position with a liquid crystal group are reported. Polymerisation of this compound produced an infusible, soluble liquid crystalline semiconducting polymer. The side-chain of the polymer had a flexible spacer of nine methylene units, terminated by a mesogenic cyanobiphenyl group. All the new compounds were chemically characterised and some were found by hot-stage polarised optical microscopy to exhibit liquid crystal mesophases. The polymer was lightly doped p-type by iodine vapour, and its electrical conductivity was measured.

Keywords: conducting   polymer,   liquid   crystal,   side-chain,   polypyrrole

1. INTRODUCTION

There is widespread interest in the properties and potential applications of liquid crystalline conjugated polymers [1-12], and pyrrole is one of the most promising building-blocks for the backbones of such polymers. However, the frequently-used 3-substituted pyrroles are nonsymmetrical monomers, effectively having a head (H) and a tail (T) [1]. Oxidative polymerisation of these molecules gives a somewhat random mixture of HH, HT, TT and TH connections between the repeating units of the polymer [1]. This causes steric crowding that will diminish the planarity and the order of the resulting polymer backbone, thus reducing its conductivity. In contrast, N-substituted pyrroles are effectively symmetrical; therefore the head and the tail are equivalent. The polymerisation of an N-substituted pyrrole (coupled regularly at the 2,5-positions) generates regioregular coupling, thereby increasing the attainable conjugation of the polymer backbone [1, 4,7].

Better organisation might be produced by attaching a liquid crystal (LC) group to the backbone of the polymer [1-7, 10-12]. In principle, this could improve the planarity and conjugation of the backbone, decrease the energy-gap and increase the mobility of the electronic charge-carriers.

In this paper we report the synthesis, polymerisation and properties of N-substituted pyrrole with a LC substituent, a strategy that has been little used [1,4,5,9].

The mesomorphic properties of a liquid crystal are determined by the nature of the mesogenic group and the linking units [13]. Cyanobiphenyl, which has proven to be stable thermally and chemically, was chosen as the primary mesogen in this work. Our previous study used a six methylene-unit spacer to favour the nematic phase [14]; in this work, a longer, nine methylene-unit spacer was chosen in order to encourage the formation of a smectic phase [13].

2. EXPERIMENTAL

Figure 1 shows the synthetic route for the preparation of the LC monomer, and the details are given below.

Thermal optical microscopy was carried out using a NIKON Optiphot-2 polarising microscope in conjunction with a Linkam THMS 600 hot-stage and TMS 91 control unit. IR spectra were measured using a Perkin-Elmer Spectrum One ATR, and

<superscript>1</superscript>HNMR spectra were recorded using JEOL Eclipse+ 400 FT-NMR (400 MHz for ^{1}H). The mass spectra were measured using a Varian 1200L Quadrupole MS. Differential scanning calorimetry (DSC) was performed on a Mettler DSC 25 instrument. A Keithley 224 current source and 617 programmable electrometer under computer control were used for 4-probe electrical conductivity measurements. X-ray diffractograms were obtained using a Bruker-AXS D-8 Advance powder X-ray diffractometer. The UV-visible spectra were measured using a Varian Cary 100 spectrophotometer.
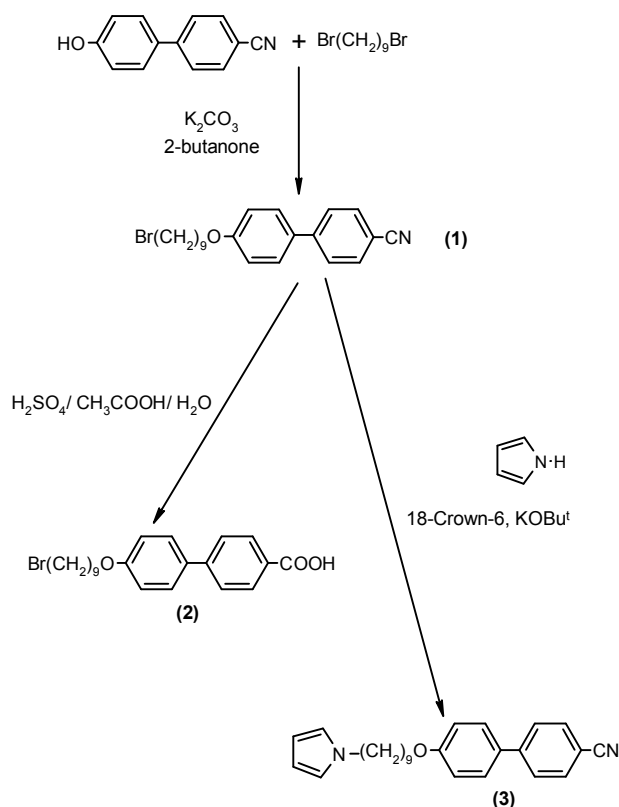

Figure 1. The synthetic route.

2.1. Synthesis of 1-bromo-9-(4-cyano-4'-biphenyloxy) nonane, compound 1

4-Cyano-4'-hydroxybiphenyl (0.98g, 5 mmol) was added to a solution of 1,9-dibromononane (6.58 g, 23 mmol) and anhydrous potassium carbonate (3.17g, 23 mmol) in 2-butanone (60 mL); the mixture was refluxed for 21h. The reaction mixture was filtered and the solvent evaporated from the filtrate under reduced pressure. The residue was recrystallised from methylated spirit and purified by column chromatography (CHCl$_3$ on silica). (Overall yield, based on 4-cyano-4'-

hydroxybiphenyl: 1.12 g, 56%); mp 66 $^{\circ}$C. MS: m/z =399 and 401 (M^{+}). FT-IR (KBr disk) υ_{max}/cm^{-1}: 2200 (CN), 1600 (C=C, Ar), 1245 (C-O-C).

^{1}H NMR (400 MHz, CDCl$_{3}$): 8.00-8.10 (d, 2H, ArH); 7.50-7.60 (d, 4H, ArH); 7.49-7.36 (d, 2H, ArH); 3.93-4.01 (m, 2H, -CH$_{2}$-O); 3.33-3.36 (t, 2H, -CH$_{2}$-Br); 1.70-1.89 (m, 14H, -CH$_{2}$-CH$_{2}$-) ppm.

2.2. Synthesis of 1-bromo-9-(4-biphenyloxy-4'-carboxylic acid) nonane, compound 2

To a mixture of water (5 mL), 95% sulphuric acid (2.7 mL) and glacial acetic acid (19.5 mL) was added 1-bromo-9-(4-cyano-4'-biphenyloxy)nonane (0.67g, 1.68 x 10^{-3} mol). The mixture was refluxed for 24 h, filtered, washed with distilled water and then cold industrial methylated spirit (IMS) before drying. The filtration residue was recrystallised 4 times from methylated spirit; yield: 0.22g, 30%. MS: m/z = 418 and 420 (M^{+}). FT-IR (KBr disk) υ_{max}/ cm^{-1}: 1601 (C=C, Ar); 1676 (C=O of COOH); 1245 (C-O-C). ^{1}H NMR (400 MHz, CDCl$_{3}$) δ (ppm): 8.07-8.10 (d, 2H, ArH); 7.85-7.60 (d, 4H, ArH); 6.88-6.94 (d, 2H, ArH); 3.93-4.01 (m, 2H, CH$_{2}$-O); 3.33-3.40 (t, 2H, CH$_{2}$-Br); 1.71-1.83 (m, 14H, CH$_{2}$-CH$_{2}$).

2.3. Synthesis of 1-(N-pyrrole)-9-(4-cyano-4'-biphenyloxy) nonane, compound 3

To a solution of 18-crown-6 (0.53 g, 2 mmol) in dry ether (100 mL) was added potassium t-butoxide (2.24 g, 20 mmol). A calcium chloride guard tube was fitted, the mixture was stirred at room temperature and pyrrole (1.4 g, 20 mmol) was added. Stirring was continued for 15 min. 1-bromo-9-(4-cyano-4'-biphenyloxy) nonane (compound 1, 1.65 g, 4 mmol) in ether (20 mL) was added dropwise over a period of 10 min and the mixture was stirred for 50h. Water (150 mL) was then added, and the mixture was extracted with ether (2 x 50 mL). The combined organic extracts were washed with saturated NaCl solution (50 mL), then water (50 mL) and dried over anhydrous MgSO$_{4}$. The solvent was removed under reduced pressure, and the product was purified by column chromatography (CHCl$_{3}$ on silica) and recrystallised from methylated spirit; yield: (0.74 g, 48 %). mp 115 $^{\circ}$C. MS: m/z = 386 (M^{+}). FT-IR (KBr disk) υ_{max}/cm^{-1}: 2224 (CN), 1602 (C=C, Ar), 1251 (C-O-C). ^{1}H NMR (400 MHz, CDCl$_{3}$) δ (ppm): 6.06-6.07 (t, 2H, pyrrole); 6.57-6.58 (t, 2H, pyrrole); 6.9-6.94 (d, 2H, ArH); 7.44-7.48 (d, 2H, ArH); 7.56-7.64 (m, 4H, ArH);

3.91-3.96 (t, 2H, CH2-O); 3.80- 3.83 (t, 2H, CH_2-N); 1.66- 1.86 (m, 14H, CH_2-CH_2).

2.4. Synthesis of poly[N-nonyl-9-(4-cyano-4`-biphenyloxy)pyrrole]

The polymerisation of compound 3 was carried out by chemical oxidation under N_2 atmosphere. The monomer (0.38 g, 1.0 mmol) was added to a filtered solution of anhydrous $FeCl_3$ (0.32 g, 1.0 mmol) in CH_2Cl_2 (50 mL). The solution was heated at 30^oC for 1h and the oxidant residues were removed by extraction with sodium EDTA solution (2 x 50 mL, 0.1 M solution). The organic layer was washed with water (2 x 50 mL), dried ($MgSO_4$), and the solvent was removed in a rotary evaporator under reduced pressure. The residual dark brown polymer was refluxed with methylated spirit and the solution was decanted to give a darker polymer residue and a soluble part (0.27 g). FT-IR (KBr disk) υ_{max}/cm^{-1}: 2224 (CN), 1604 (C=C, Ar), 1248 (C-O-C). ^{1}H NMR (400 MHz, $CDCl_3$) δ (ppm): 6.07-6.08 (t, 2H, pyrrole); 6.57-6.58 (t, 2H, pyrrole); 6.91-6.93 (d, 2H, ArH); 7.45-7.48 (d, 2H, ArH); 7.56-7.64 (m, 4H, ArH); 3.91-3.95 (t, 2H, CH_2-O); 3.81- 3.84 (t, 2H, CH_2-N); 1.66-1.83 (m, 14H, CH_2-CH_2).

2.4. Electrochemical polymerisation

The monomer was electrochemically polymerised from a solution containing tetrabutylammonium tetrafluoroborate (TBAF; 0.14 g, 1.0 mmol) and the monomer (90 mg, 1.0 mmol) dissolved in 25 mL of dry propylene carbonate (N_2 purged). The cell consisted of a stainless steel counter electrode, an indium-tin oxide (ITO) glass working electrode and a sealed saturated calomel reference electrode. The electrode potential was cycled 40 times from -0.3 V to +1.5 V vs. SCE, at a scan rate of $50 mVs^{-1}$.

3.   RESULTS AND DISCUSSION

3.1. Electrochemistry

Figure 2 shows a cyclic voltammogram for the first five cycles of electrochemical polymerisation of the N-substituted pyrrole. The ITO glass working electrode was eventually coated with a dark brown film of polymer.
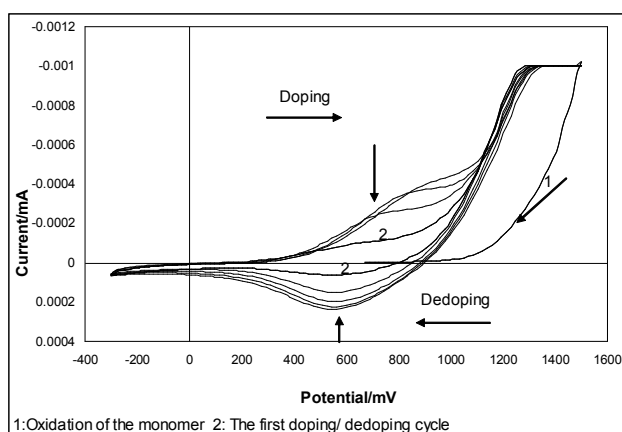
Figure 2. A cyclic voltammogram showing the redox properties of the N-substituted pyrrole; scan rate 50 mV.s⁻¹.

In the first half-cycle, oxidative polymerisation of the monomer started at 1200mV vs SCE; the subsequent reduction (dedoping) of the resulting orange polymer film was observed at about 600mV. As would be expected, redoping of the polymer occurred at lower potential (ca. 750mV) than that for monomer oxidation. In the following oxidative half-cycle, the polymer film thickness (and hence the anodic current) increased. The colour of the film gradually changed to very dark brown as the cycling continued to form a coherent film of polymer.

The doping occurred at progressively higher potential in the successive oxidative stages, probably because the dedoped film resistance was becoming more significant after each cycle. In contrast, the cathodic dedoping potential remained quite constant because the oxidised films were reasonably conductive.

The electrochemical oxidation and reduction of the as-grown polymer occurred at higher potentials than that for polypyrrole (by ca. 350mV). This is probably due to the steric effects of the un-aligned LC group, decreasing the effective conjugation length and hence increasing the ionisation potential of the polymer backbone.

3.2. Molecular modelling

Quantum Cache © software (Fujitsu Limited) was used to predict the optimised local arrangement of the atoms in an isolated molecule of the monomer. Figure 3 depicts an optimised structure for the monomer, which suggests that the mesogen and the spacer are not collinear with the pyrrole unit.
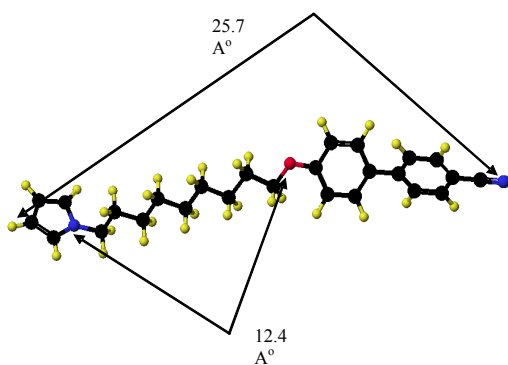
Figure 3. The N-substituted pyrrole monomer.

On this simple basis, without consideration of intermolecular forces or the effects of polymerisation, the length of the monomer with LC group attached is 25.7 Å. After adding the van der Waals radii of the C≡N nitrogen and the pyrrole hydrogen (respectively 0.92 and 1.2 Å) to the length of the monomer, the effective length is 27.8 Å. This result is very close to the long spacing distance obtained by X-ray diffractometry (section 3.5). The polymer was studied as well, and the results matched those of the isolated monomer.

3.3. Polymer characterisation

Figure 4 shows the UV-visible spectrum of a thin polymer film on ITO glass, following electrochemical synthesis and dedoping. It features a strong π-π^* peak at 300nm, an absorption edge at 442nm (2.8 eV) and a very weak peak at 890 nm indicating polaron absorption due to slight residual doping. The energy gap (2.8 eV) is slightly larger than that of an analogous polymer with a shorter spacer of six methylene units (2.5 eV) [1], and lager than that of unsubstituted polypyrrole [3].

However, after mild annealing of the sample at 135 $^{\circ}$C in vacuum for 2 h, the energy gap decreased to 2.6 eV; this is thought to be due to the self-organisation of the smectic liquid crystal phase, leading to a more planar backbone.

Films of the polymer were lightly doped by exposure to a mild oxidant, iodine vapour, for 24 h at ambient temperature. The electrical conductivity of this doped polymer was measured using the four-probe method to be 2.8×10^{-6} S m^{-1}. This is less than that (1.3×10^{-4} S m^{-1}) of the polymer with a shorter spacer[1], which may be due to lighter doping, or to the longer spacer increasing the steric hindrance.
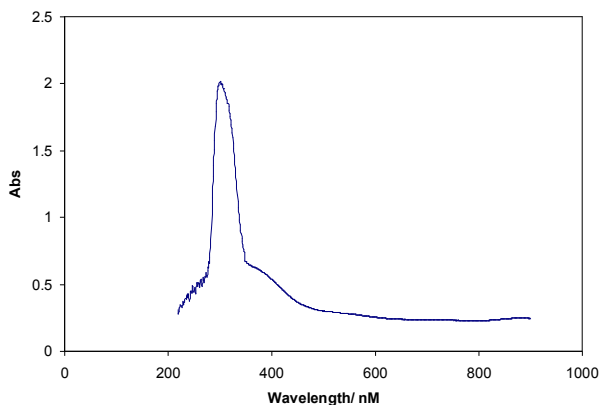
Figure 4. UV-visible spectrum of a dedoped film of the
polymer on silica glass.

3.4. Liquid crystal (LC) Properties

The transition temperatures for all monomers and the polymer were studied by differential scanning calorimetry (DSC) and hot-stage polarising microscopy. For compounds 1 and 3, only a normal melting point was observed, These results are unlike those of a previous study of compounds analogous to 1 and 3 (with shorter spacers) which exhibited a nematic phase[1]. Compound 2 (the acid) showed both a nematic and a smectic C phase, C→S_C 144.8 $^{\circ}$C, S_C→N 186.5 $^{\circ}$C, N→I 241.4 $^{\circ}$C, S_C→C 147.0 $^{\circ}$C.

The nematic phase of compound 2 as it changed from isotropic to nematic was homeotropic in appearance on a large proportion of the slide which flashed when a mechanical pressure was applied to the slide. A polarised optical micrograph texture is shown in Figure 5.
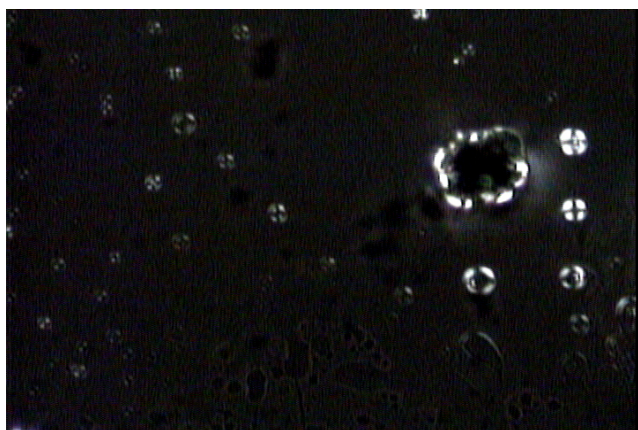

Figure 5. Polarised hot-stage micrograph of compound 2 showing a bright appearance around the air bubbles in the homeotropic texture of the nematic phase at 229.1°C.

Under the microscope, the phase changed again at 186.5 ^{o}C to a schlieren texture. It was identified to be a smectic C phase, since (a) the phase no longer flashed and (b) the texture showed only four associated brushes, unlike the nematic phase which shows centres with two brushes. The colour of the texture changed with temperature from white to yellow-brown to blue on cooling. This is consistent with the observations of Gray and Goodby [14] for the schlieren texture of the smectic C phase with a colour change from yellow-grey to yellow-brown and finally to blue, due to the tilt angle changes occurring as the temperature decreases. The acid crystallised at 147.0 ^{o}C. A micrographic texture of the S_c phase is given in Figure 6.
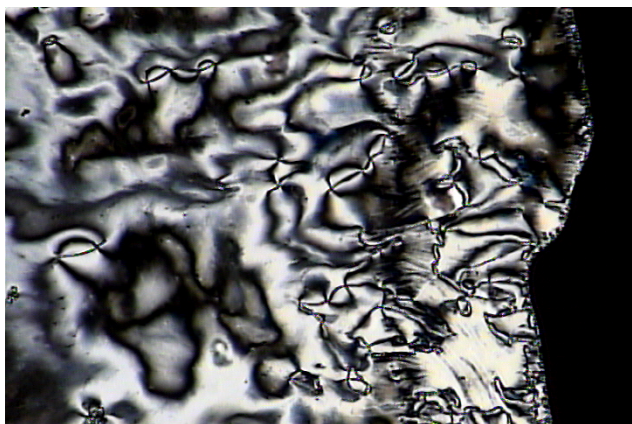

Figure 6. Polarised hot-stage micrograph of compound 2 showing the schlieren texture of the smectic C phase at 179.1 ^{o}C.

The DSC trace of the polymer showed one peak, in addition to the glass transition. By studying the polymer under hot-stage microscopy, a phase was distinguished after holding the polymer at 136.3 ^{o}C for 30 min. This phase was further developed on holding the sample at 111.5 ^{o}C for another 30 min. The complex texture developed slowly, and it is believed to be due to a highly organised liquid crystal mesophase; work is still in progress to characterise it. Figures 7 and 8 show developed optical textures of the polymer at different temperatures.
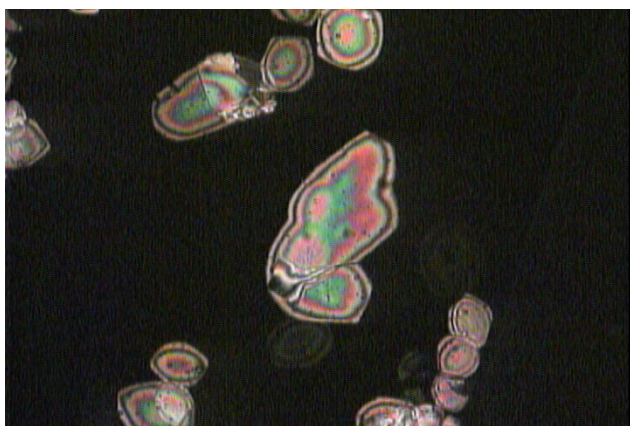
Figure 7. Polarised hot-stage micrograph of the polymer showing the texture exhibited after holding the sample at 136.3 ^{o}C for 30 min.
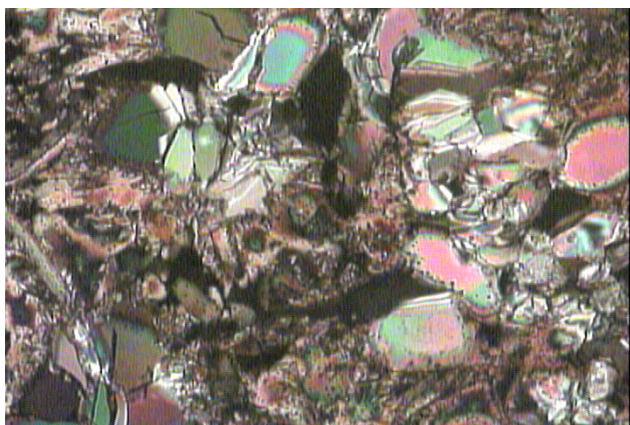

Figure 8. Polarised hot-stage micrograph of the polymer showing the texture that developed after holding the sample at 111.5 ^{o}C for 30 min.

3.5. X-ray diffractometry

Figure 9 shows X-ray diffractograms for both a powder and a pressed pellet of the polymer. One can distinguish three fairly sharp peaks in the pattern of the pellet, while there was just one peak in the case of the powder (Table 1 shows the corresponding d-spacings). This suggests that compressing the polymer increased the packing efficiency of the polymer, and therefore favoured crystalline or liquid crystalline organisation of the molecules.
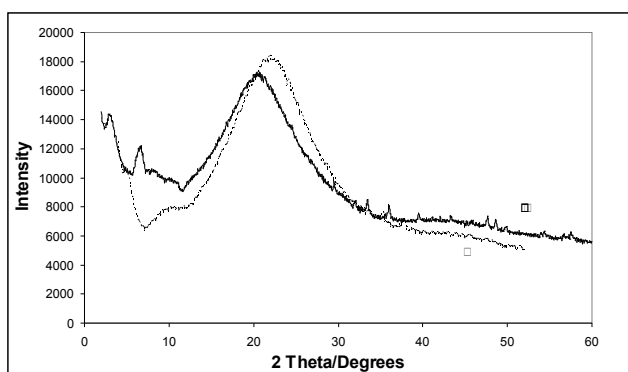
Figure 9. X-ray diffractograms of the polymer as: [] a powder and [II] a pellet.

Table 1. XRD data for the LC polymer

Peak No.	Powder d/Å	Pellet d/Å	Proposed Assignment
1	4.4+/- 0.04	4.32+/- 0.04	Inter-monomer spacing
2	-	14.0 +/- 0.1	Possibly 2nd order peak
3	-	27.6 +/- 0.3	Smectic phase inter-layer spacing

The peak at 4.6 Å (4.32 Å in the pellet) is similar to one which is dominant for most polypyrrole samples, and is thought to relate to the broad range of cofacial repeat distances between the monomer units [15]. The enhanced peak showing a long spacing of 27.6 Å is comparable with the van der Waals length of a fully-extended monomer-spacer-mesogen unit, and so it is proposed that this is the interlayer spacing of the smectic LC phase indicated by hot-stage polarised optical microscopy (Section 3.4). Within experimental error, peak no. 2 at 14.0 Å could be assigned as a 2nd–order reflection of this.

4. CONCLUSIONS

In this paper, the synthesis of new liquid crystal compounds is reported. The acid intermediate (product 2) showed two liquid crystal mesophases. A nematic and a smectic C mesophase were observed to be stable over a wide range of temperature. The pyrrole monomer was polymerised both chemically and electrochemically, and the redox properties of the resulting polymer were studied. The polymer has a larger

energy gap and lower conductivity than one with a shorter spacer. Mild annealing of the polymer gave a lower energy gap due the LC self-organisation and likely to produce significantly increased conductivity. Modelling the monomer using Quantum Cache/Scigress software indicated molecular dimensions consistent with the repeat distances indicated by X-ray diffractometry. A well-organised texture was observed by polarised optical microscopy while holding the polymer at high temperature. Work is continuing to characterise the mesophase of the polymer fully, and to study effects of an applied magnetic field and thermo-optic alignment on the organisation and the conductivity of the polymer.

REFERENCES

1   G.J. Lambe, J.W. Brown and P.J.S. Foot (2006). Liquid Crystal Conducting Polymers, in "Specialty Polymers – Materials & Applications", ed. F. Mohammad, IK International Publishers, 2-18..

2   K. Akagi (2007). Synthesis and Properties of Liquid-Crystalline-Conjugated Polymers. *Bull. Chem. Soc. Jpn.*, **80**, 649–661.

3   S. Yang and C. Hsu (2009). Liquid Crystalline Conjugated Polymers and their Applications in Organic Electronics. *Polymer Chemistry*, **47**, 2713–2733.

4   Yu Chen, C. T. Imrie and K S. Ryder, *J. Mater. Chem.*, **11**, (2001) 990-995.

5   M. Kijima, S. Abe and H. Shirakawa, *Synth. Met.*, **101**, (1999) 61.

6   S. Cosnier and A. Senillou, Chem. Commun, 2003, 414-415.

7   J. W. Brown, P. J. S. Foot, L. I. Gabaston, P. Ibison and A. Prevost, *Macromol. Chem. Phys.*, **205**, (2004), 1823-1828.

8   Yu Chen, William T. A. Harrison, Corrie T. Imrie and Karl S. Ryder, *J. Mater. Chem.*, **12**, (2002), 579-585.

9   Yu Chen, C. T. Imrie and K. S. Ryder, *J. Mater. Sci. Lett.*, **21**, (2002), 595-597.

10   D. Roudini, *Polymers and Polymer Composites*, **25**, (2017) 643-649.

11   B. P. J. de L Costello, N. M. Ratcliffe and P. S. Sivanand, *Synth. Met.*, **139**, (2003), 43-55.

12   K. Masuda, K. Akagi, H. Shirakawa and T. Nishizawa, *J. Molec. Struct.*, **441**, (1998), 173-181.

13   J. Collings and M. Hird, *Introduction to Liquid Crystals (Chemistry and Physics)*, ed. G. W. Gray, J. W. Goodby and A. Fukuda; Taylor & Francis, London (1997).

14   P. Ibison, P. J. S. Foot and J. W. Brown, *Synth. Met.*, **76**, (1996), 297.

15   G. W. Gray and J. W. Goodby, *Smectic Liquid Crystals*; Leonard Hill, London (1984).

16   B. Street, T. C. Clarke, R. H. Geiss, V. Y. Lee, A. Nazzal, P. Pfluger and T. C. Scott, *J. Phys. (Paris) Colloq.*, **44**, (1983), C3-599.

17   I. McCulloch, M. Heeney, C. Bailey, et al, *Nature Materials* 5, (2006) 328-333.

18   X. Li, L. Chen, Y. Chen, F. Li and Kai Yao. *Organic Electronics*, **13**, (2012) 104–113.

19   W. Chen, Y. Chen, F. Li, L. Chen, K. Yuan, K. Yao, P. Wang. *Solar Energy Materials and Solar Cells*, 96, (2012), 266–275.